Proceedings of the
International Conference on Mechanical Engineering 2005
(ICME2005) 28- 30 December 2005, Dhaka, Bangladesh

ICME05-TH-18

MODELING OF FLUIDIZATION CHARACTERISTICS OF QUARTZ SAND IN A CONE-SHAPED BED OF A BIOMASS COMBUSTOR

Rachadaporn Kaewklum and Vladimir I. Kuprianov

School of Manufacturing Systems and Mechanical Engineering, Sirindhorn International Institute of Technology, Thammasat University, P.O. Box 22, Thammasat Rangsit Post Office, Pathumthani, 12121, Thailand.

ABSTRACT

This paper deals with the modeling of the major fluidization characteristics of quartz sand ($SiO_2 \approx 90\%$)in a conical bed. Some modifications to the models related to the partially fluidized bed mode are proposed. The minimum fluidization velocity, the minimum velocity of full fluidization as well as the dependence of the pressure drop (across the bed) on the superficial velocity (related to the bottom bed section) are presented for the sand particles of the 300–500 μm size passed by the flow of air under ambient conditions. Effects of the cone angle and static bed height on the fluidization pattern as well as on the above characteristics are discussed. The predicted dependencies of the pressure drop versus superficial velocity for different cone angles (30^o, 44^o and 60^o) and bed heights (20, 30 and 40 cm) are discussed in comparison with reference experimental data for similar operating conditions. As found in this work, the computational error deteriorates for the greater cone angles and static bed heights.

Keywords: Minimum fluidization velocity; Minimum velocity of full fluidization; Pressure drop.

1. INTRODUCTION

The fluidized bed technology has been widely used in many industrial processes. The minimum fluidization velocity, u_{mf}, and the pressure drop across the bed, Δp, are the major input data for designing an atmospheric non-circulating fluidized-bed system. Together with the terminal velocity, u_t, which is an important parameter in the designing of a circulating fluidized bed system, these fluidization characteristics are basically used for determining the reactor's dimensions, selecting auxiliary equipment (e.g. blower) and predicting the range of major operating variables for the system to be developed.

By present time, a large number of research works devoted to modeling the fluidization characteristics of a gas-solid fluidized bed have been carried out on cylindrical and prismatic devices, or columns, operating under "cold" (ambient) conditions [1–4]. For different particle and fluidizing agent properties/characteristics, the behaviors of solid particles in the fluidized bed are represented by corresponding fluidization patterns (bubbling, slugging, channeling and jetting). In practical fluidized bed systems, the group-B and group-D particles are generally used with the aim of securing the bubbling fluidization mode in the particular device, as follows from the Geldart's particle classification [1]. Accordingly, u_{mf} and Δp are affected by the fluidization pattern, the latter being dependent on the particle size. Hence, for the selected bed material, the particle size seems to be another important parameter for the proper designing of fluidized bed systems and, accordingly, for simulation of the fluidized bed.

A large group of the fluidized bed systems include the reactors (devices) with cone-shaped and tapered beds [5–9]. As shown by different authors, the bed geometry affects significantly both the fluidization mode (e.g. causing the bed spouting at large cone angles) and the fluidization characteristics [1], particularly, for coarse particles [5]. With the use of the same bed material, one can observe different fluidization modes occurring at different cone angles. Moreover, the effects of the static bed height of the conical bed become more apparent compared to those in columns. As concluded in some references, in addition to the above characteristics, the minimum velocity of full fluidization, u_{mff}, should be involved for more complete characterization of the conical and tapered fluidized beds [5,6].

The models for predicting $u_{mf,}$ u_{mff} and Δp (the latter being the function of the superficial velocity) have been proposed and applied for the cases of liquid fluidizing agent as well as for reactors with coarse particles (of about 1.8 mm diameter) of the bed material [5,6]. However, there is a lack of reliable data on fluidization characteristics for the bed materials with medium particle size, typical for fluidized bed combustion systems including those with the conical bed [10,11].

This work was aimed at modeling $u_{mf,}$ u_{mff} and Δp for the conical bed filled in with the quartz sand, of 300–500 μm in size, passed by the flow of air under ambient

conditions. Effects of the cone angle and static bed height on these characteristics were the focus of study. Validation of the computational models was also among the main objectives of this study.

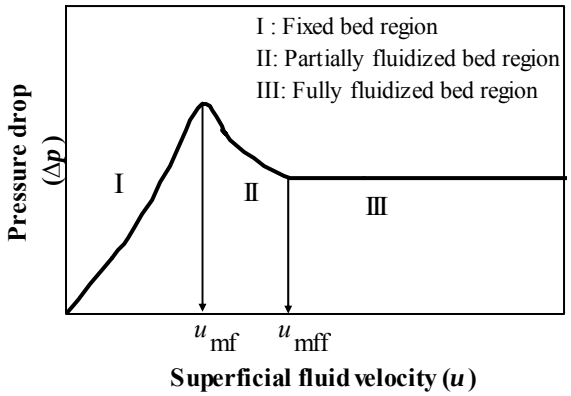

Fig 1. Effect of the superficial fluid velocity on the pressure drop across the conical (or tapered) bed [5,6].

2. METHODS AND MATERIALS

2.1 Computational Models

A typical relationship between the pressure drop (across the conical/tapered bed) and the superficial velocity in the bed (basically, related to the bottom section) is shown in Fig. 1. Apparently, this dependence can be subdivided into three regions corresponding to different modes: (I) fixed bed mode (occurring at $u < u_{mf}$), (II) partially fluidized bed mode (at $u_{mf} \le u < u_{mff}$), and (III) fully (turbulent) fluidized bed mode (at $u \ge u_{mff}$) [5,6]. For a spouted bed, Δp may reduce in Region III with higher u [1].

In accordance with the work objectives, a conical fluidized bed system is the focus of the study. The schematics diagram of the conical bed prototype is shown in Fig. 2.

Fixed bed mode (Region I). In such a mode, solid particles of the bed material are fixed (in contact with neighboring particles) forming the static bed of height h as shown in Fig. 2.

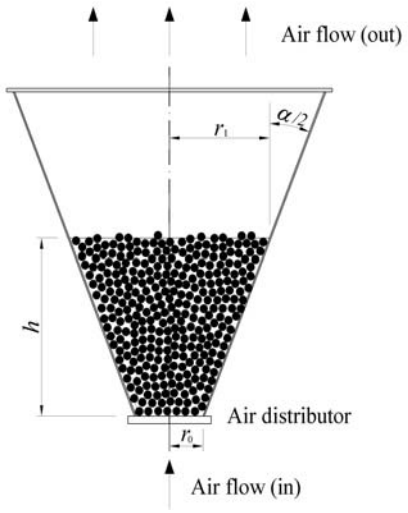

Fig 2. Schematic diagram of the conical bed filled in with the bed material (fixed bed mode).

For determining the superficial velocity range for this region, the value of u_{mf} is required. The equation for quantifying u_{mf} is derived based on the assumption that for $u = u_{mf}$ (occurring at the bed voidage $\varepsilon = \varepsilon_{mf}$ [1]) the buoyancy force acting on the entire bed is in equilibrium with the net gravitational force of all the bed particles [6]:

$$A u_{mf} + B \frac{r_0}{r_1} u_{mf}^2 - (1-\varepsilon_{mf})(\rho_s - \rho_f) g \frac{r_0^2 + r_0 r_1 + r_1^2}{3 r_0^2} = 0 \tag{1}$$

where

$$A = 150 \frac{(1-\varepsilon_{mf})^2}{\varepsilon_{mf}^3} \frac{\mu_f}{(\phi_s d_p)^2} \tag{2}$$

and

$$B = 1.75 \frac{1-\varepsilon_{mf}}{\varepsilon_{mf}^3} \frac{\rho_f}{\phi_s d_p} \tag{3}$$

In Region I, laminar air flow may likely occur between the bed particles, especially when the particle size is relatively small. In such a case, basically taking place at $Re_{mf} < 20$, the viscous effects in the air flow crossing the bed become predominant, and all the term with u^2_{mf} in Eqs. (1) can be omitted, hence simplifying the determining of u_{mf} [2].

For the conical bed at $u < u_{mf}$, i.e. when $\varepsilon = \varepsilon_o$, the pressure drop across the bed is determined for various u by the modified Ergun's equation [6]:

$$\Delta p = A h \frac{r_0}{r_1} u + B h \frac{r_0 \left(r_0^{\,2} + r_0 r_1 + r_1^{\,2} \right)}{3 r_1^{\,3}} u^2 + \frac{1}{2} \left(\frac{u}{\varepsilon_0} \right)^2 \left[\left(\frac{r_0}{r_1} \right)^4 - 1 \right] \rho_f \tag{4}$$

where A and B are calculated by Eq. (2) and Eq. (3), respectively, replacing ε_{mf} by ε_o.

As follows from analysis of Eq. (4), the pressure drop approaches the maximum (Δp_{max}) at $u = u_{mf}$.

Partially fluidized bed region (Region II). When the partially fluidized bed mode occurs, some part of the bed of a height h_b ($h_b < h$) with the particles near the air distributor shows the fluidization mode, whereas the particles in upper bed layers remain to be static as illustrated in Fig. 3.

For determining the upper velocity limit for this region (u_{mff}), basically occurring at $\varepsilon = \varepsilon_{mff}$, the condition of the equality of the buoyancy force acting on the upper layer of the fluidized bed (with an infinitesimal thickness) to the gravity force acting on that layer must be satisfied. Such a conditions results in the following equation suitable for quantifying the minimum velocity of full fluidization [6]:

$$A\left(\frac{r_0}{r_1}\right)^2 u_{\text{mff}} + B\left(\frac{r_0}{r_1}\right)^4 u_{\text{mff}}^2 - (1-\varepsilon_{\text{mff}})(\rho_s - \rho_f)g = 0 \quad (5)$$

where A and B are calculated by Eq. (2) and Eq. (3), respectively, replacing ε_{mf} by ε_{mff}.

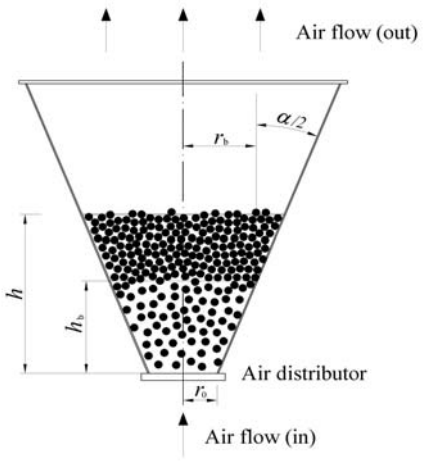

Fig 3. Schematic diagram of the conical bed filled in with the bed material (partially fluidized bed mode).

In this work, it was suggested to estimate the value of h_b as the function of the current superficial velocity:

$$h_b = \frac{u - u_{\text{mf}}}{u_{\text{mff}} - u_{\text{mf}}} h \quad (6)$$

Hence, the radius of the top plane of the fluidized part, r_b, is then readily found to be:

$$r_b = r_0 + \left[h_b \tan\left(\frac{\alpha}{2}\right)\right] \quad (7)$$

In the fixed part of the partially fluidized bed, the bed voidage is characterized by the same, as in Region I, value, i.e. $\varepsilon = \varepsilon_o$. Meanwhile, in the bed part with the fluidization (of height h_b), the bed voidage is proposed to correlate with the current superficial velocity by:

$$\varepsilon = \varepsilon_{\text{mf}} + \left(\frac{u - u_{\text{mf}}}{u_{\text{mff}} - u_{\text{mf}}}\right)^{0.5} (\varepsilon_{\text{mff}} - \varepsilon_{\text{mf}}) \quad (8)$$

The pressure drop across the bed for this region of $u_{\text{mf}} \le u < u_{\text{mff}}$ is then calculated to be [6]:

$$\Delta p = A(h-h_b)\frac{r_0^2}{r_1 r_b} u + B(h-h_b)\frac{r_0^4\left(r_b^2 + r_b r_1 + r_1^2\right)}{3 r_1^3 r_b^3} u^2 + (1-\varepsilon)(\rho_s - \rho_f)g h_b + \frac{1}{2}u^2\left[\left(\frac{1}{\varepsilon_0}\right)^2\left(\frac{r_0}{r_1}\right)^4 - \left(\frac{1}{\varepsilon}\right)^2\right]\rho_f \quad (9)$$

where A and B are calculated by Eq. (2) and Eq. (3), respectively, replacing ε_{mf} by ε, the latter being found by Eq. (8).

Note that the contribution of the last term in Eq. (9) (related to the kinetic energy change) is quite negligible and can be omitted in practical applications.

With higher u, the pressure drop in the partially fluidized bed region is reduced approaching a minimum at $u = u_{\text{mff}}$, i.e. when $h = h_b$. Under such a condition, the terms with A and B in Eq. (9) are turned to be zero.

Fully fluidized bed region (Region III). In accordance with the above analysis, the pressure drop across the bed in this region is represented by the third term on the right site of Eq. (9) whose value is independent of u. Assuming that the bed voidage to be constant value in Region III ($\varepsilon \approx \varepsilon_{\text{mff}}$), the pressure drop is then estimated by:

$$\Delta p = (1 - \varepsilon_{\text{mff}})(\rho_s - \rho_f)gh \quad (10)$$

2.2 Essential Input

For validation of the computational models, all calculations in this work were carried out for the same, as in Ref. [11], bed material (quartz sand) and fluidizing agent (air, under ambient conditions). Properties and characteristics of both quartz sand and air used in this computational study are shown in Table 1. The voidage of the fixed bed was assumed by Ref. [1] for the loosely packed bed; meanwhile, the values of ε_{mf} and ε_{mff} were selected based on the reference experimental data [11].

Table 1: Properties and characteristics of quartz sand and air used in the computational study

Property/characteristic	Value
SiO_2 content in the quartz sand	89.9% (by wt.)
Diameter of sand particles, d_p	400 μm
Density of sand, ρ_s	2650 kg/m^3
Sphericity of sand particles, φ_s	0.86
Density of air, ρ_f	1.165 kg/m^3
Viscosity of air, μ_f	$1.86 \cdot 10^{-5}$ N·s/m^2
Voidage of the fixed bed, ε_o	0.46
Voidage of the bed at the minimum fluidization velocity, ε_{mf}	0.46
Voidage of the bed at the minimum velocity of full fluidization, ε_{mff}	0.49

In accordance with the work objectives, the computations of the fluidization characteristics were carried out for the conical prototype, as shown in Fig. 1, with different cone angles (30, 44 and 60°) but fixed bottom base diameter (25 cm). For each prototype, the computations were repeated for three values of the (static) bed height: 20, 30 and 40 cm.

3. RESULTS AND DISCUSSION

Figures 4 and 5 show the predicted dependencies of the pressure drop on superficial air velocity for the bed heights of 20 and 30 cm, respectively, for distinct cone angles.

As seen in Figs. (4) and (5), in Region I, the predicted $\Delta p = f(u)$ seems to be rather linear than of the second order, especially for the smallest bed height (20 cm). This fact indicates the predominance of the viscous effects at relatively low superficial velocities of air flow.

The value of u_{mf} was found to depend on the cone angle showing stronger effects with higher bed heights. Thus, for the bed height of 20 cm, the predicted u_{mf} were found to be 0.29, 0.34 and 0.42 m/s (see Fig. 4) for the cone angles of 30, 44 and 60°, whereas they were 0.35, 0.45 and 0.56 m/s (see Fig. 5), respectively, when the bed height was 30 cm. Apart from this, the computational results showed the influence of the cone angle on the Δp_{max} which increased with higher cone angles, and this effect was more apparent for higher bed heights.

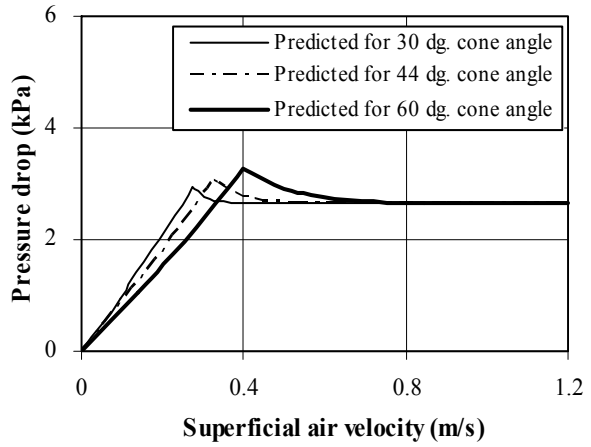

Fig 4. Predicted pressure drop across the conical bed versus superficial air velocity for the static bed height of 20 cm at different cone angles

However, the experimental work on the conical prototypes with the particles of 0.3–0.4 mm in diameter [11] provided the conclusion on the independence of u_{mf} on the cone angle. For the bed height of 20 cm, the experimental u_{mf} was found to be about 0.34 m/s and was apparently regardless of the cone angle, whereas for the bed height of 30 cm, the experimental u_{mf} ranged from 0.34 to 40 m/s when the cone angle was varied from 30 to 60°. These differences in u_{mf} could be explained by the conditions of the sand packing (loosely packed particles).

Meanwhile, the experimental results with coarse (1.8 mm diameter) particles proved the substantial effects of the cone angle on both u_{mf} and Δp_{max} [5], corresponding qualitatively to the above conclusions.

In addition, Figs. 3 and 4 show quite strong effects of the cone angle on the characteristics of Region II, particularly, on u_{mff}. Again, this fact has found the qualitative confirmation for the coarse particles [5].

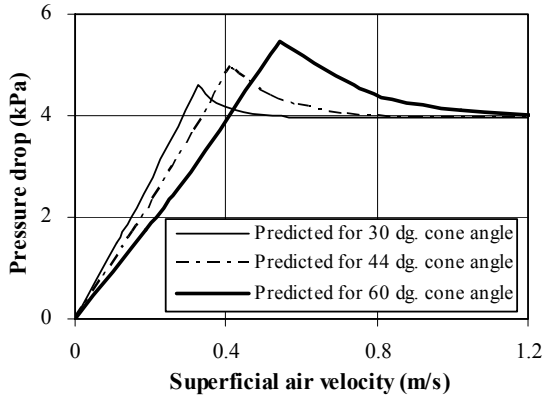

Fig 5. Predicted pressure drop across the conical bed versus superficial air velocity for the static bed height of 30 cm at different cone angles.

Figures 6, 7 and 8 depict the predicted and experimental dependencies $\Delta p = f(u)$ for the conical prototypes with the 30, 44 and 60° cone angles, respectively, for two static bed heights, of 20 and 30 cm. Because of loosely packed sand particles in the tests [11], the predicted and empirical dependencies (for the same operating conditions) seen to be quite far, particularly, in Region II. Despite these differences, one can observe some certain trends in data compared.

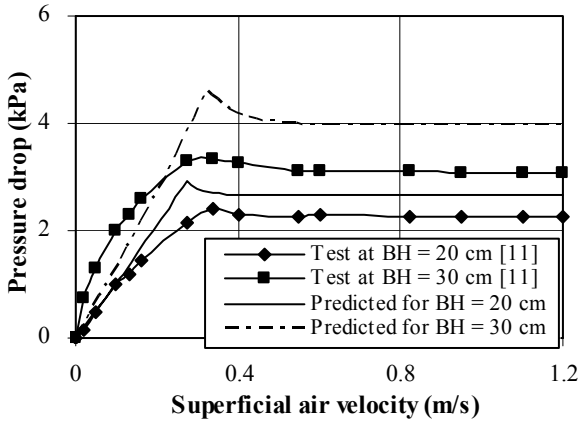

Fig 6. Comparison of predicted and experimental data on the pressure drop across the conical bed with the 30° cone angle for different static bed heights

For all the cases (under above operating conditions), the predicted and experimental Δp were found to be in good agreement for low superficial velocities of air flow ($u < 0.2$ m/s). This fact points at the correct selection of the ε_o which is, in effect, an important parameter in the models.

Since the model for Region I, i.e. Eq. (4), provides a solution "for the tightly packed bed", the predicted and experimental dependencies are diverged at $0.2 \le u \le u_{mf}$, the most significant differences being observed at $u = u_{mf}$. These differences have the trend to enhance with higher static bed heights. Despite the difference in the pressure drop, the predicted and experimental u_{mf} were found to

be in good (for the 30° cone angle) or fair (for greater cone angles) agreement.

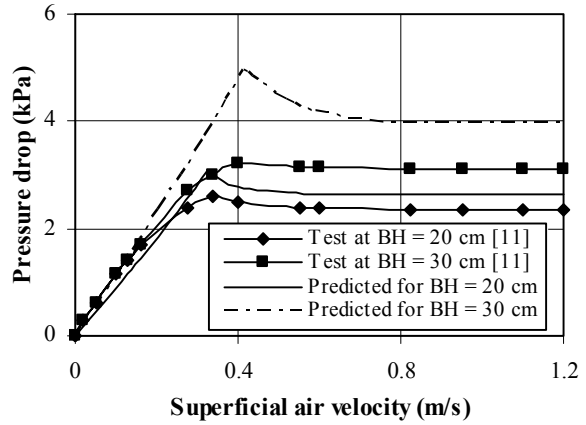

Fig 7. Comparison of predicted and experimental data on the pressure drop across the conical bed with the 44° cone angle for different static bed heights.

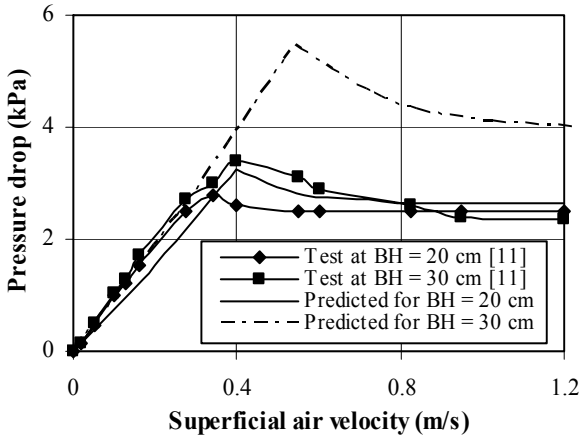

Fig 8. Comparison of predicted and experimental data on the pressure drop across the conical bed with the 60° cone angle for different static bed heights.

The fluidization characteristics of Region III are of the highest interest since they are used in the criteria for developing the reactor's design. Thus, for providing secured fluidization for wide range of the reactor loading, the actual operating velocity should be selected as high as (6–10)u_{mff}. Based on this value and taking into account the air distributor geometrical characteristics, the ranges for the air volume flow rate can be then estimated. The pressure drop for this region is also one of the factors affecting the selection of the blower(s).

As seen in Figs. 6–8, for the bed height of 20 cm, the predicted u_{mff} and Δp (for $u > u_{mff}$) were found to be in rather good agreement with the corresponding experimental results, remaining within 10–20% band (depending on the cone angle). However, with higher bed height and/or cone angle, relative computational errors for u_{mff} and Δp become substantially higher. For instance, for the cone angle of 44°, both errors approach approximately 30%.

4. CONCLUSIONS

Computational models were successfully applied for predicting the fluidization characteristics, the minimum fluidization velocity (u_{mf}), the minimum velocity of full fluidization (u_{mff}), as well as the dependence of the pressure drop (Δp) on the superficial air velocity (u) for the conical bed filled in with quartz sand. The models have been validated by comparison the predicted results with reference data for various cone angles of the conical prototype at different static bed heights.

For the fixed bed mode (occurring at $u < u_{mf}$), the modified Ergun's equation used in this work provided the reliable predictions for low superficial air velocities ($u <$ 0.2 m/s). Meanwhile, the minimum fluidization velocity obtained from the experiment was found to be higher.

For the partially fluidized bed mode (at $u_{mf} \le u < u_{mff}$), the predicted and experimental results were found to be quite different because of loosely packed bed in the experimental tests. These differences became stronger with higher bed height (showing major effect) and cone angle (showing minor effect).

For the fully fluidized bed mode (for $u > u_{mff}$), the predicted u_{mff} and Δp were found to be in rather good agreement with the corresponding experimental results, remaining within 10–20% band (depending on the cone angle). However, with higher bed height and/or cone angle, the relative computational errors for u_{mff} and Δp became substantially higher.

5. REFERENCES

1. Geldart, D., 1986, *Gas Fluidization Technology*, John Wiley & Sons, New York.
2. Kunii, D. and Levenspiel, O., 1991, *Fluidization Engineering*, Butterworth-Heinemann, Boston.
3. Caicedo, G. R., Ruiz, M. G., Marqués, P. and Soler, J. G., 2002, "Minimum Fluidization Velocities for Gas-Solid 2D Beds", Chemical Engineering and Processing, 41: 761−764.
4. Ergun, S., 1952, "Fluid Flow Through Packed Columns", Chemical Engineering Progress, 48:89−94.
5. Jing, S., Hu, Q., Wang, J. and Jin,Y., 2000, "Fluidization of Coarse Particles in Gas-Solid Conical Beds", Chemical Engineering and Processing, 39: 379−387.
6. Peng, Y. and Fan, L. T., 1997, "Hydrodynamic Characteristics of Fluidization in Liquid-Solid Tapered Beds", Chemical Engineering Science, 52(14): 2277−2290.
7. Olazar, M., San José, M.J, Aguayo, A.T., Arandes, J.M. and Bilbao, J., 1992, "Stable Operation Condition for Gas-Solid Contact Regimes in Conical Spouted Beds", Industrial and Engineering Chemistry Research, 31(7):1784−1798.
8. Bi, H. T., Macchi, A., Chaouki, J. and Legros, R., 1997, "Minimum Spouting Velocity of Conical Spouted Beds", The Canadian Journal of Chemical Engineering, 75:460−465.
9. Cui, H., Mostoufi, N. and Chaouki, J., 2000, "Characterization of Dynamics Gas-Solid Distribution in Fluidized beds", Chemical

Engineering Journal, 79:133−143.
10. Permchart, W. and Kouprianov, V. I., 2004, "Emission Performance and Combustion Efficiency of a Conical Fluidized-Bed Combustor Firing Various Biomass Fuels", Bioresource Technology, 92: 83−91.
11. Permchart, W. and Kouprianov, V. I., 2004, "Fluidization Characteristics of a Conical Sand Bed", *Proc. 15th International Symposium on Transport Phenomena*, pp. 461−466.

6. NOMENCLATURE

Symbol	Meaning	Unit
A	Constant in the modified Ergun's equation	($N \cdot s/m^4$)
B	Constant in the modified Ergun's equation	(kg/m^4)
d_p	Diameter of sand particles	(m)
g	Gravity acceleration	(m/s^2)
h	Static bed height	(m)
h_b	Height of the fluidized region in the partially fluidized bed	(m)
Δp	Pressure drop across the bed	(kPa)
Δp_{max}	Maximum pressure drop across the bed (at $u = u_{mf}$)	(kPa)
Re_{mf}	Reynolds number determined at the superficial velocity u_{mf}	(-)
r_o	Radius of the lower base of the conical bed	(m)
r_1	Radius of the upper base of the static bed	(m)
r_b	Radius of the upper base of the fluidized bed (for the partially fluidized mode)	(m)
u	The fluidizing velocity through the entrance of the particle bed (i.e. at the lower bed base)	(m/s)
u_{mf}	Minimum fluidization velocity	(m/s)
u_{mff}	Minimum velocity of full fluidization	(m/s)
α	Cone angle	(^{o})
ε	Current bed voidage (for the partially fluidized mode)	(-)
ε_o	Bed voidage for the fixed bed mode	(-)
ε_{mf}	Bed voidage at the minimum fluidization velocity	(-)
ε_{mff}	Bed voidage at the velocity of full fluidization	(-)
ϕ_s	Sphericity of bed material (sand) particles	(-)
ρ_s	Density of the bed particles	(kg/m^3)
μ_f	Viscosity of the fluidizing agent (air)	($N \cdot s/m^2$)
ρ_f	Density of the fluidizing agent (air)	(kg/m^3)